Cloud frequency climatology at the Andes/Amazon transition: 2. Trends and variability

Kate Halladay,[1] Yadvinder Malhi,[1] and Mark New[1,2]

Received 15 March 2012; revised 23 September 2012; accepted 4 October 2012; published 1 December 2012.

[1] The climate and ecology of tropical montane systems is intimately connected with the complex spatial dynamics of cloud occurrence, but there have been few studies of the patterns and trends of cloud occurrence in tropical montane regions. We examine trends and variability in the cloud climatology of the Andes/Amazon transition in SW Amazonia using satellite data and ground-based observations. Results were compared for three zones within the study area: highlands (puna grassland), eastern slope (Tropical Montane Cloud Forest or TMCF) and lowlands. Time series of cloud frequency from ISCCP (International Satellite Cloud Climatology Project) were correlated with sea surface temperature (SST) anomalies from the HadISST data set for 5 regions including the tropical North Atlantic and the tropical Pacific. Detrended lowland cloud frequencies were significantly correlated with detrended tropical North Atlantic SSTs in the late dry season (August/September), whereas the eastern slope and the highlands were not significantly correlated with tropical North Atlantic SSTs. Pacific SST correlations were highest for eastern slope and highlands from March to May. Indian Ocean SST anomalies were significantly correlated with dry season cloud frequency for the lowlands and highlands. There are significant decreasing trends in cloud frequency on the lowlands in January, March and September and in March on the eastern slope. Trends in sunshine duration, 850 hPa zonal winds over the central Amazon, increases in diurnal temperature range, and comparisons with MODIS (Moderate Resolution Imaging Spectroradiometer) and observational data support the existence of these trends, and a link with the increasing trend in tropical North Atlantic SSTs. We suggest that continued increases in tropical North Atlantic SSTs will further reduce cloud frequency in the lowlands adjacent to the TMCF in the late dry season at least. In addition, a future increase in the occurrence of El Niño events would lead to decreased cloud frequency on the eastern slope and highlands.

Citation: Halladay, K., Y. Malhi, and M. New (2012), Cloud frequency climatology at the Andes/Amazon transition: 2. Trends and variability, *J. Geophys. Res.*, *117*, D23103, doi:10.1029/2012JD017789.

1. Introduction

[2] Tropical Montane Cloud Forests (TMCFs) may be defined by their almost constant immersion in cloud, resulting from a combination of climatological factors. They tend to be distributed in narrow zones where prevailing winds meet the topography which forces ascent and consequent cloud formation. The distribution and the specific adaptation of species to the high frequency of cloud immersion lead to high levels of endemism and biodiversity. In the context of current climate change, the vulnerability of TMCFs to modifications in temperature, humidity and circulation needs to be explored.

[3] A number of studies suggest that TMCFs are already affected or are likely to be affected by climate change [e.g., *Foster*, 2001; *Pounds et al.*, 1999]. Sea surface temperature (SST) increases are implicated by *Pounds et al.* [1999] in causing an increase in cloud height by decreasing the temperature lapse rate and thereby increasing the Lifting Condensation Level (LCL) height (a proxy for cloud base height), with specific reference to the Monteverde cloud forest in Costa Rica. The effect of SSTs on the lapse rate is likely to be more applicable to TMCFs in oceanic settings than those in continental settings such as the eastern flank of the Andes. With reference to the Amazon, *Pinto et al.* [2009] suggest that decreased SSTs also increase the LCL height by reducing the amount of evaporation from the sea surface and thus moisture transport from the tropical ocean to the Amazon. Rather than investigating the likely effect of temperature changes on cloud height, this study examines cloud frequency, as changes in cloud height on a slope increase cloud frequency in one location and decrease it at

[1]Environmental Change Institute, School of Geography and the Environment, University of Oxford, Oxford, UK.
[2]African Climate and Development Initiative, University of Cape Town, Rondebosch, South Africa.

Corresponding author: K. Halladay, Environmental Change Institute, School of Geography and the Environment, University of Oxford, South Parks Road, Oxford OX1 3QY, UK. (kate.halladay@ouce.ox.ac.uk)

0148-0227/12/2012JD017789

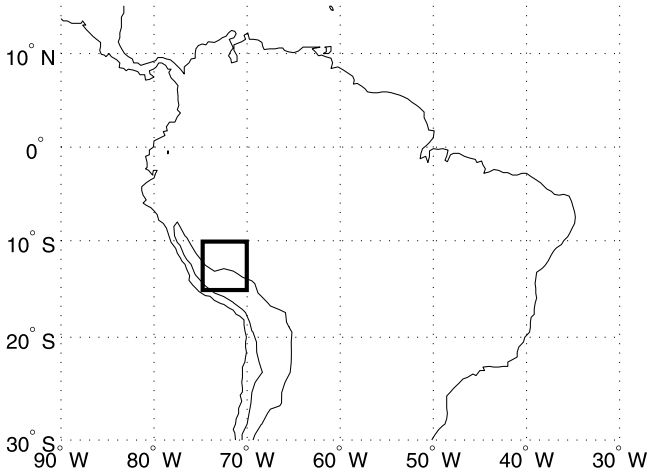

Figure 1. Map to indicate location of 5 degree by 5 degree box containing the study area (enclosed by thick black line). Terrain above 3000 m altitude is enclosed by a contour line.

another. It also considers changes in circulation in addition to temperature as possible causes.

[4] The TMCF and surroundings at the focus of this study is the Kosñipata Valley, the location and specifics of which are described in *Halladay et al.* [2012]. This area lies at the transition between the high Andes and the lowland Amazon Basin; therefore, the climate of the study area exhibits similarities with both of these zones (Figure 1). The study area was one of four areas along the eastern slopes of the Andes that were categorized by *Killeen et al.* [2007] as super-humid regions on account of the relative orientation of prevailing winds and topography. It was argued that this makes them climatically stable. However, evidence for circulation variability on interannual or decadal timescales has not been previously considered.

[5] Most research relevant to clouds and climate in the region of interest concentrates on convective cloud and precipitation in either the central Andes or lowland Amazonia. In the central Andes it is well known that upper level zonal winds have a strong influence on precipitation variability on diurnal to interannual timescales [e.g., *Garreaud*, 1999; *Vuille*, 1999; *Vuille and Keimig*, 2004]. *Vuille and Keimig* [2004] show that the controls on interannual variability differ between northern and southern regions of the Altiplano (15 to 21°S), notably that low-level moisture conditions over the lowlands to the east are of little significance to the variability of northern regions (close to study area). Rossby waves from the extratropics are known to play a role in influencing the position and strength of zonal wind anomalies [*Lenters and Cook*, 1999; *Vuille et al.*, 1998]. The influence of Pacific SSTs and ENSO has been shown by *Vuille* [1999] to manifest in strengthened upper easterlies for high phases of ENSO (La Niña) and the reverse for low phases (El Niño). *Vuille et al.* [2000] extended this work by showing that Atlantic, in addition to Pacific SSTs, influence summer precipitation and temperature variability in the central Andes. The role of topography in addition to the SST-driven large scale circulation was emphasized by *Giovannettone and Barros* [2009] in a study investigating controls on convective cloudiness in southern Peru and the central Andes. It was shown that the nighttime patterns of cloudiness were more influenced by local circulations associated with the topography, and less by interannual variability in the large-scale circulation, but the reverse was found for daytime patterns.

[6] Research into the climate of the lowland Amazon indicates the importance of Atlantic SSTs in influencing rainfall variability [*Cox et al.*, 2008; *Liebmann and Marengo*, 2001; *Yoon and Zeng*, 2010], and in particular on their role in causing the 2005 drought [*Marengo et al.*, 2008]. It has long been established that ENSO has a profound influence on the interannual variability of the large-scale circulation of the South American region. *Marengo and Hastenrath* [1993] summarized the features of the circulation and SST anomalies associated with wet and dry years (in March/April) in the Amazon Basin, remarking that the features of wet (dry) years were similar to those of La Niña (El Niño) years, although the wet and dry anomalies were not limited to extreme ENSO indices. The role of Atlantic SSTs relative to ENSO depends on the time of year [*Yoon and Zeng*, 2010; *Zeng et al.*, 2008], but the longevity of SST anomalies often leads to a combined effect from both regions [*Ronchail et al.*, 2002]. Although it has been asserted that ENSO is responsible for 50–80% of the anomalous SST variability in the tropical Atlantic [*Enfield and Mayer*, 1997], it has its own mechanisms of variability that are independent of ENSO, e.g., the "Atlantic Niño" which is not correlated with ENSO [*Xie and Carton*, 2004]. More recently, Indian Ocean SSTs have also been implicated in influencing precipitation variability by *Drumond and Ambrizzi* [2008].

[7] Trends and interannual variability in cloud frequency over the lowland Amazon were examined by *Arias et al.* [2011], who found decreasing trends in total cloud in DJF and SON which were supported by trends in outgoing longwave radiation. The trends were linked to SSTs in the Atlantic and western Pacific, leading to increased subsidence, reduced moisture flux and anomalous wave trains. Trends in cloud frequency over global land areas have also been reported by *Warren et al.* [2007]. The trends were derived from surface observations for the period 1971–1996. Most areas showed a decrease in cloud frequency but the greatest rate of decrease was reported for South America. Trends in cloudiness from ISCCP data by season (1984–2006) were also investigated by *Butt et al.* [2009] with reference to the whole Amazon basin and 5 sub-regions within it. For the whole region, decreasing trends were significant in the dry season, with an increase in February. One of the sub-regions included the Andes/Amazon transition but was too large to separate localized trends from regional trends.

[8] *Halladay et al.* [2012] found differences in the cloud climatology in three zones across the Andes/Amazon transition and found that eastern slope was an area of higher cloud frequency and lower variability. The highlands showed the greatest amplitude annual cycle with an earlier minimum cloud frequency than on the eastern slope and the lowlands. Interannual variability and trends in cloud frequency were not explored.

[9] There therefore remains a gap in understanding of differences in controlling influences on cloud frequency variability across the Andes/Amazon transition, in particular, the influences on cloud as distinct from rainfall or convective cloud, which are mostly a wet season phenomenon in this region. However, the TMCF ecosystem is likely to be more sensitive to cloud frequency in the dry season than in the wet

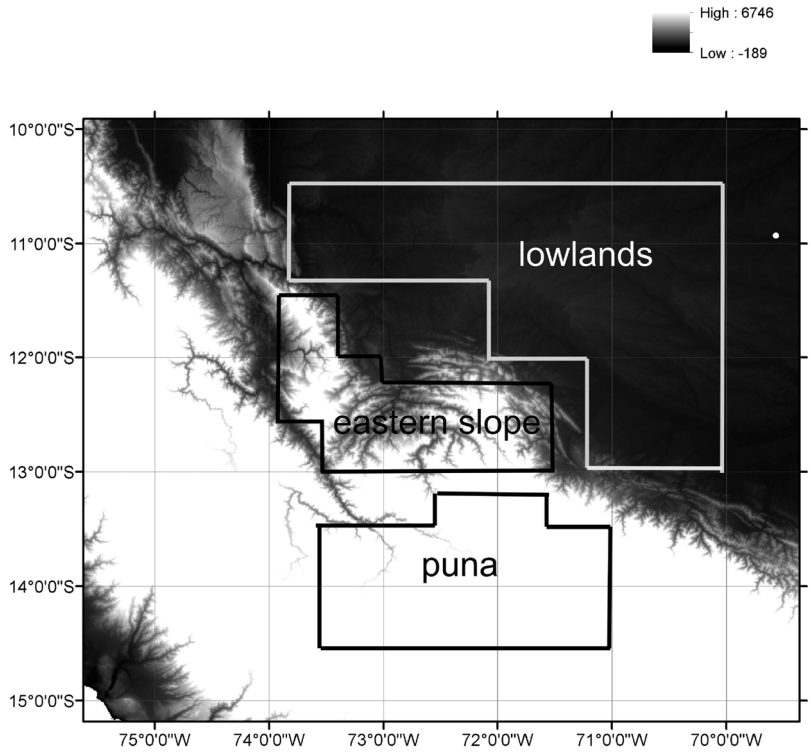

Figure 2. Lowlands, eastern slope and puna areas within area 10 to 15°S and 75 to 70°W as derived from the *Mulligan and Burke* [2005] map of cloud forest distributions are enclosed by solid lines. Elevations are in meters.

season when moisture is not a limiting factor. Region-specific impacts of recent changes in climate on cloud frequency have also not been quantified. In order to understand the impacts of recent climate change on the cloud distributions in the study area and in the wider context of the tropical Andes and Amazon, this study aims to (1) characterize the covariation of cloud frequency for the highland (puna), slope and lowland zones, (2) examine the links with SSTs, (3) investigate the major controlling mechanisms governing variability, and extent to which they differ between the three zones and (4) quantify and explain temporal trends in cloud frequency and possible controlling mechanisms.

2. Data and Methods

2.1. Satellite Observations of Cloud Frequency

[10] Data from the International Cloud Climatology Project [*Rossow and Schiffer*, 1991, 1999] DX product at approximately 30 km and 3-hourly resolution covering the period 1983 to 2008 were used to estimate cloud frequency after the application of a viewing angle correction. This procedure corrects for the over-estimation of cloud amounts that occurs with oblique viewing angles. The DX product includes binary cloud flags (cloudy/cloud-free), latitude and longitude and viewing angle for each pixel. Cloud flags and viewing angles were averaged for each month in the data period. The correction procedure used slope and intercept values obtained by plotting cloud amounts from two geostationary satellites against each other for periods common to both satellites. These values were used to adjust cloud amounts for periods with non-orthogonal viewing angles. Full details of the DX product, the viewing angle correction procedure and data processing are described in *Halladay et al.* [2012].

[11] In this study, ISCCP data were extracted from a 5 by 5 degree area in order to examine the relationship between SSTs and cloud frequency and any long-term trends in the 3 zones. An area of this size was chosen to include enough pixels to obtain a robust measure in each zone, to maximize the correlations between cloud frequencies and SSTs, and to enable the viewing angle correction procedure to be applied to an area of a size for which it had been tested.

[12] In order to extract pixels that were representative of the 3 zones within the 5 by 5 degree area of ISCCP data, a mask was generated from a map of cloud forest distributions available at http://www.ambiotek.com/cloudforests [*Mulligan and Burke*, 2005], and used to define areas of puna, eastern slope and lowlands within a 5 degree by 5 degree area (Figure 2). The eastern slope region defined within the 1 degree area [*Halladay et al.*, 2012, Figure 1] was found to cover approximately the same area as "current fractional cloud forest cover greater than 90%" in the map produced by *Mulligan and Burke* [2005].

2.2. Other Data

[13] Cloud amount observations in oktas from two surface stations at Chontachaca (13.02°S, 71.47°W, elevation: 982 m) and Rocotal (13.11°S, 71.57°W, elevation: 2010 m) were obtained from the Peruvian meteorological service (Senamhi). These were available for the period from January 2000 to December 2008 at 1200, 1800 and 0000 UTC (0700, 1300 and 1900 local time). If any days from a month were missing, data from that month were excluded from the time series. The total

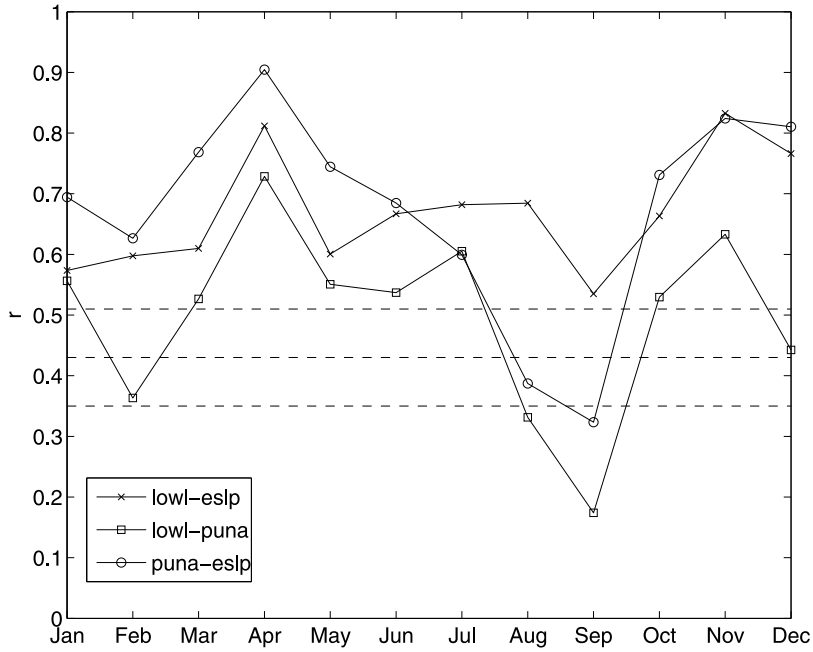

Figure 3. Correlation coefficient for cloud frequency time series for each pair of zones by month. Dotted lines represent the 1%, 5% and 10% significance levels.

missing observations amounted to 1% for Chontachaca, and 13% for Rocotal.

[14] Sea surface temperature data were obtained from the HadISST data set (http://hadobs.metoffice.com/hadisst/) [*Rayner et al.*, 2003] at 1 degree spatial resolution and monthly temporal resolution, based on SST measurements from the UKMO Marine Data Bank, available from 1870 to present.

[15] NCEP-NCAR reanalysis data [*Kalnay et al.*, 1996] were extracted to aid in the interpretation of cloud frequency trends. These data are available at a 6-hourly and 2.5 by 2.5 degree resolution, for the period 1948 to present.

3. Results

3.1. Covariability Between Zones

[16] The covariability in cloud frequency for each pair of zones is investigated to indicate whether they are subject to common mechanisms of variability and whether the same relationships persist throughout the annual cycle. The data from all times of day were averaged within each zone to get a value for each month and corrected for viewing angle changes before correlation. The three zones are correlated on an annual basis with $r \sim 0.65$ for the eastern slope and the lowlands and puna on either side, and $r = 0.49$ for the lowlands and puna. However, the r value is subject to variation through the annual cycle (Figure 3). Most notable is a peak in covariability in April and a minimum in September which are common to all three pairings. High correlations would be expected in the wet season as cloud frequencies are high in all 3 zones [*Halladay et al.*, 2012] associated with the predominance of upper level easterlies promoting upslope flow and convection across the study area. In the late dry season (August/September) only the lowlands and eastern slope remain significantly correlated, but the puna is decoupled from the other zones, suggesting that controls on cloud frequency variability differ from those in the wet season.

3.2. Link With SSTs

[17] Interannual variability of climate in the tropics is known to be dominated by SSTs in tropical oceans; however, the nature of this association within the study area has not been explored. Hence, the cloud frequency anomaly time series derived from the ISCCP data in a 5×5 degree box containing the study area was correlated with global SST anomalies. It was found that the strongest correlations were located in the TNA, the Indian Ocean and three areas of the Pacific. Monthly time series of cloud frequency from the three zones were detrended (i.e., best fit linear trend removed from the data) then correlated with areal mean SST anomalies (also detrended) for these areas (Figure 4).

[18] The values of the correlation coefficient (r) by month are plotted in Figure 5. For the puna, the eastern Pacific regions and Indian Ocean SSTs were most strongly correlated with cloud frequency, with strongest correlations in the late wet season and early dry season (March to June). The r values for the tropical Pacific were approximately -0.60 from March to May, indicating that high eastern tropical Pacific SSTs (El Niño conditions) are associated with reduced cloud frequency on the puna, in agreement with *Vuille*'s [1999] study of precipitation over the Altiplano. In some months of the dry season, the Indian Ocean SSTs were significantly correlated (at the 5% level) with cloud frequency. Partial correlation of Indian Ocean SST anomalies with cloud frequency controlling for tropical Pacific and TNA SST anomalies indicated that for the puna, the relationship was still significant in June and February.

[19] The association of SST anomalies in the Indian Ocean with South American climate has recently been documented by

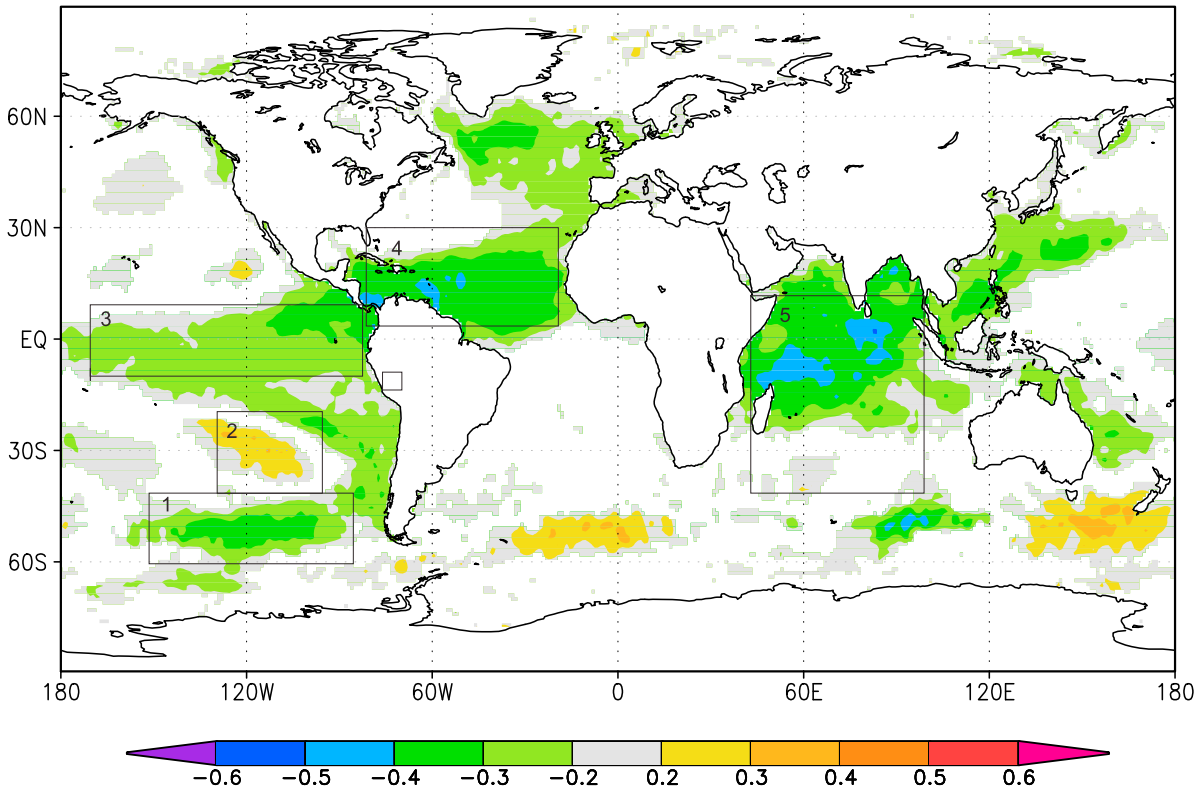

Figure 4. Correlation (r) values of ISCCP DX mean monthly cloud frequency standardized anomaly 1983–2008 for 10 to 15°S, 75 to 70°W (p-values above 0.1 are masked out) with HadISST anomalies for same period. Position of 5 degree box is indicated by a black box (not numbered) and SST areas are numbered 1 (South Pacific), 2 (South Pacific Anticyclone), 3 (Tropical Pacific), 4 (Tropical Atlantic) and 5 (Indian Ocean).

Drumond and Ambrizzi [2008]. They describe a mechanism by which the SST anomalies can force Rossby Waves along an arc-like path across the South Pacific toward South America, constrained by the upper-level jet stream. With higher SSTs the upper level pressure pattern acts to weaken the surface pressure gradient and hence the strength of the Trade winds, which in turn reduces the moisture flux and cloud frequency.

[20] SST anomalies in the South Pacific anticyclone area were significantly correlated in February, October, and in May, July and August with opposite sign to the tropical Pacific, i.e., high SSTs correlate with high cloud frequency. High (low) SSTs in the South Pacific anticyclone area may increase (decrease) the SST gradient between the central Pacific and the coastal waters and thus increase the surface pressure gradient and strengthen (weaken) the anticyclone. SON composites (not shown) of the 850 hPa wind anomalies from months with high and low SST anomalies in this region confirmed the strengthening and weakening of the anticyclone. The anticyclone may not exert a direct influence on cloud frequency on the puna but is likely to form part of a more widespread mode of SST variability via teleconnections.

[21] The correlation coefficients for the eastern slope are broadly similar to those of the puna. However, there were some differences for the eastern slope: the correlation with the Indian Ocean was weaker in the dry season, but stronger with the tropical Pacific in SON.

[22] For the lowlands, most significant correlations were found with the Indian Ocean and TNA SSTs. The strongest correlations (approximately −0.50) occurred in February, July, August, September and December. In the late dry season North Atlantic SSTs reach their boreal summer peak in while austral winter Pacific SSTs are lower. Hence, the signal from the Atlantic is likely to dominate. Higher SSTs over tropical oceans tend to enhance local ascent, which results in enhanced descent over the continents to compensate [*Cox et al.*, 2008]. The late wet season correlation may reflect an Atlantic response to SST anomalies in the Pacific, as has been reported by *Xie and Carton* [2004]. Other teleconnection patterns exist between the different SST regions; however, partial correlations of Indian Ocean SSTs controlling for tropical Pacific and TNA SST anomalies indicated that from June to August, the correlation is still significant.

[23] Lag/lead correlations of cloud frequency for the three zones and SSTs from all regions with lags/leads of up to six months did not indicate the presence of any dominant lag effects.

[24] Correlations were also performed before detrending for the TNA and tropical Pacific regions and for each zone. The effect of including the trend on the r values was greatest for the lowlands (Table 1). The correlation coefficients for the TNA are higher by at least 0.1 when the trend is included for 7 months of the year, with the greatest differences in January, March and September. However, in September, the increase in r attributable to the trend was relatively small as a proportion of r(detrend) data, whereas in January r(detrend) was almost negligible at −0.06, but the inclusion of the trend

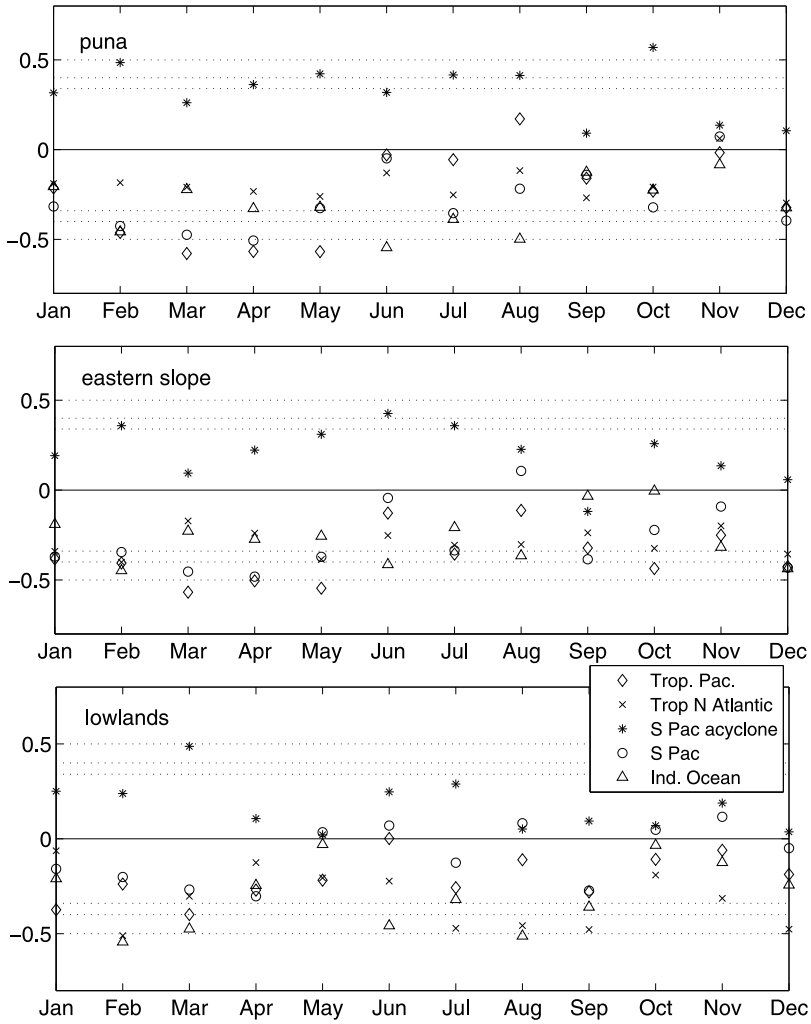

Figure 5. Correlation coefficients by month of mean cloud frequency anomalies for 3 zones with SST anomalies for 5 areas (detrended). Dotted lines represent 10, 5 and 1% significance levels.

made r significant at the 5% level. Detrending the data had little effect on the correlations with the tropical Pacific, except in March when r(detrend) was significant at the 5% level.

[25] The results of the correlations including and excluding trend for the eastern slope and puna are shown in Tables S1 and S2 in the auxiliary material.[1] For the puna, the TNA r values were reduced by up to 0.17 with the trend included in February, July, October and December but increased by up to 0.14 in January, June and November. On the eastern slope inclusion of the trend increased r by 0.23 in March, but reduced it by 0.16 in October. Tropical Pacific r values were altered by less than 0.05 for both the puna and eastern slope. If the r values become significant after the inclusion of a trend, it suggests that common trends in the two time series may be coincidental, and therefore only r(detrend) should be considered when assessing correlation. Although TNA r values in the lowlands for several months are increased by inclusion of the trend, r is still significant in the mid to late dry season suggesting that SSTs affect cloud frequency at that time of year.

[26] The relationship between cloud frequencies in the three zones and SSTs in the TNA and tropical Pacific is qualitatively represented in Figure 6. The period from 1983 to 1990 (labeled A) was characterized by large interannual

Table 1. Correlation Coefficients (r) for Monthly HadISSTs for the TNA and Tropical Pacific and Cloud Frequencies for the Lowlands

	Tropical N Atlantic			Tropical Pacific		
	Detrended	W/ Trend	Diff.[a]	Detrended	W/ Trend	Diff.[a]
Jan	−0.06	−0.42	**−0.36**	−0.37	−0.31	0.07
Feb	−0.51	−0.52	−0.01	−0.24	−0.23	0.01
Mar	−0.30	−0.58	**−0.27**	−0.40	−0.32	0.08
Apr	−0.13	−0.28	**−0.16**	−0.27	−0.28	−0.01
May	−0.21	−0.39	**−0.19**	−0.22	−0.22	0.00
Jun	−0.22	−0.21	0.01	0.00	0.00	−0.01
Jul	−0.47	−0.38	0.10	−0.26	−0.26	0.00
Aug	−0.46	−0.57	**−0.12**	−0.11	−0.12	−0.01
Sep	−0.48	−0.69	**−0.21**	−0.28	−0.22	0.06
Oct	−0.19	−0.09	*0.10*	−0.11	−0.10	0.00
Nov	−0.31	−0.46	**−0.15**	−0.06	−0.08	−0.02
Dec	−0.48	−0.41	0.06	−0.19	−0.20	−0.01

[a] r diff. (=r (trend) − r (detrend)). R diff values less (greater) than 0.1 are shown in bold (italic).

[1] Auxiliary materials are available in the HTML. doi:10.1029/2012JD017789.

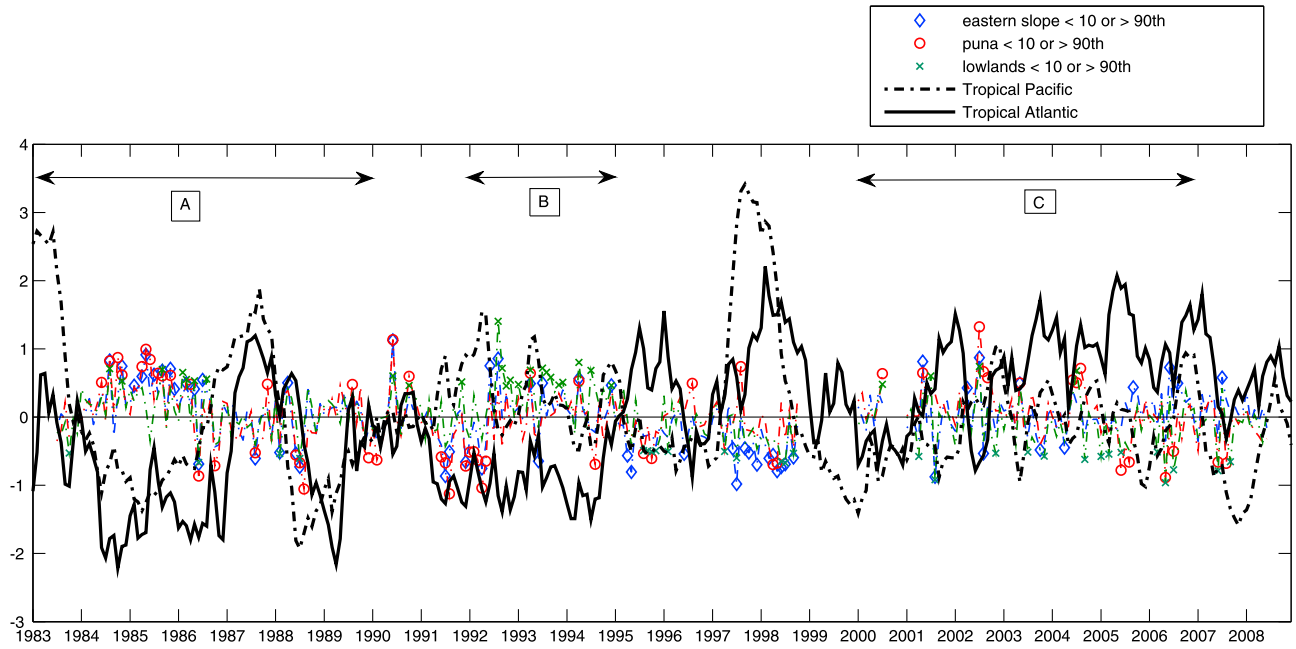

Figure 6. Standardized anomalies of cloud frequency for the 3 zones (gray dashed lines) and standardized SST anomalies in °C for tropical Pacific (dashed black line) and TNA (solid black line). Red circles mark puna cloud frequencies below the 10th percentile and above the 90th percentile, blue diamonds mark the same for the eastern slope, and green crosses mark the same for the lowlands.

variability in the tropical Pacific and includes the 1987 El Niño event. SST anomalies in the TNA tend to follow those in the tropical Pacific after an ENSO event. Around 1985 to 1986 both were low, and cloud frequencies were high for all three zones, then as both SST areas entered a period of warm anomalies in 1987 all three zones experienced low cloud frequency anomalies. From 1992 to 1995 (labeled B), Pacific SST anomalies were mostly warm, and cloud frequencies on the puna were low, while in the TNA they were mostly cool, and cloud frequencies in the lowlands were high. When SST anomalies in the TNA became warm in 1995, cloud frequencies in the lowlands changed sign. During the 1997/1998 El Niño, cloud frequencies were low in all 3 zones. From 2002 to 2007 (labeled C), SST anomalies in the TNA remained warm throughout, and cloud frequencies in the lowlands were low while tropical Pacific SSTs showed low-amplitude fluctuations. Note that the SST anomalies in the TNA showed a significant increasing trend for the period shown in Figure 6 but tropical Pacific SSTs showed no trend; these SSTs trends are considered in more detail in Section 4.4.1

3.3. SST Anomaly Composites

[27] In order to explore the circulation features that are associated with SST anomalies in the TNA and the tropical Pacific areas shown in Figure 6, composite maps for each combination of high and low SST anomalies in the two regions were generated. High SST anomalies were assigned to a season when the anomaly was positive or zero in all three months of the season and low when all 3 months showed negative or zero anomalies. Anomaly maps for SSTs, cloud frequency, upper and low level circulation and moisture flux for the transition seasons MAM and SON are shown in Figures 7 and 8. These seasons have been chosen as the impact of changes in cloud frequency during these seasons has a greater potential to affect the TMCF ecosystem by lengthening the dry season, during which clouds are an important source of moisture. The SST anomalies in each basin, cloud frequency anomalies in the three zones, and circulation and moisture flux anomalies in the study area for each composite and all seasons are listed in Table 2.

[28] In MAM (Figures 7a and 7b) there is a clear pattern of low (high) cloud frequencies over much of the Amazon south of the equator when SST anomalies in the TNA and tropical Pacific are both high (low). Anomalies in the upper level flow are southwesterly (northeasterly) with high (low) SSTs in the tropical Pacific, and appear dominant in determining the sign of the cloud frequency anomalies on the puna and the eastern slope (Table 2). The direction of upper-level zonal flow has been shown to be important in determining convective cloud and rainfall variability in the central Andes [e.g., *Vuille and Keimig*, 2004] and is correlated with cloud frequency on the puna and eastern slope in MAM. When the TNA and tropical Pacific SST anomalies are of the same sign, the effect extends to the lowlands. Low-level wind anomalies are consistent with those at upper levels, in that upper westerly anomalies occur with low-level northwesterly anomalies. *Garreaud* [1999] suggests that strengthened northwesterlies along the eastern side of the central Andes, and in particular SALLJ episodes, reduce upslope flow due to Coriolis deflection away from the slope. This may explain the low cloud frequency anomalies on the eastern slope and puna (Figures 7a and 7c). Lowland cloud frequency anomalies are low (high) when TNA SST anomalies are high (low), although the low and upper-level circulation anomalies change direction with the tropical Pacific SSTs.

[29] However, in the case of opposite anomalies in the tropical Pacific and TNA, positive (negative) TNA SST anomalies occur with negative (positive) moisture flux

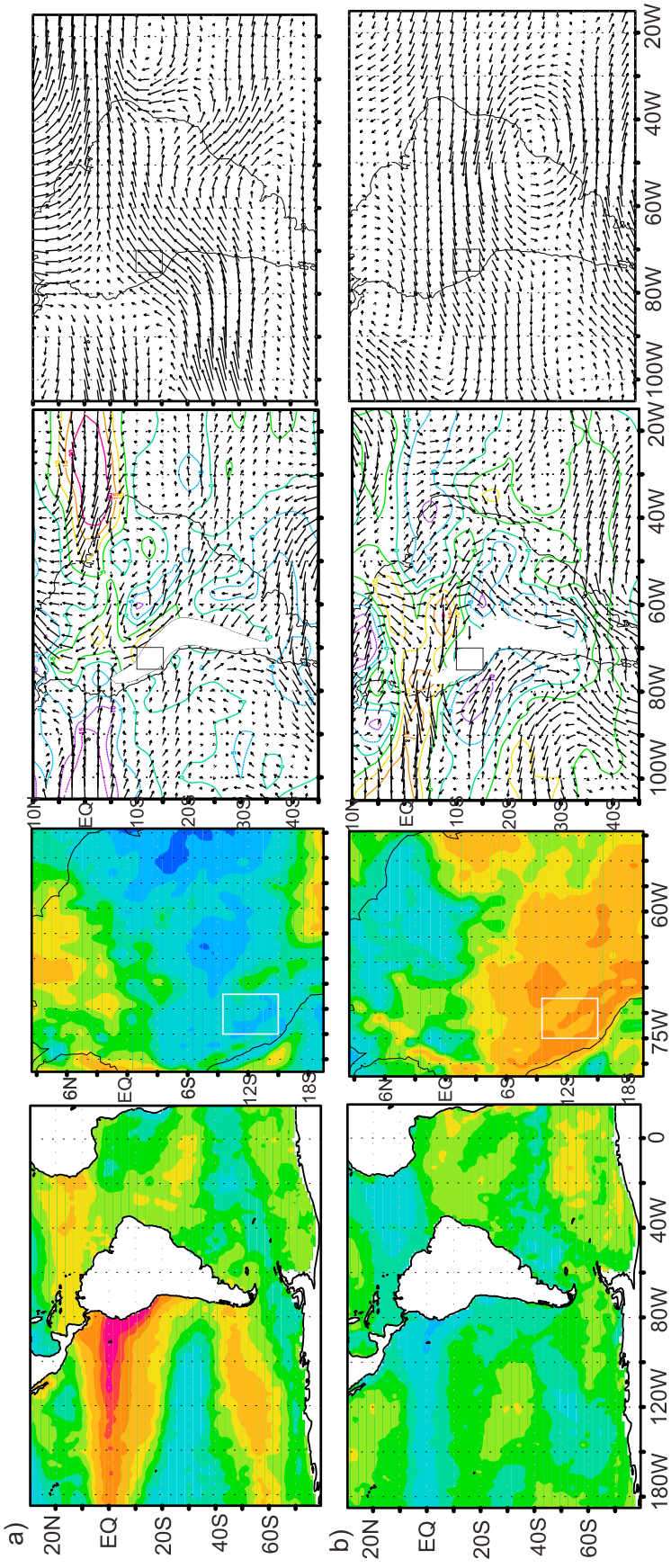

Figure 7. MAM anomalies for HadISST (3-month moving average applied), ISCCP cloud frequency, NCEP/NCAR reanalysis 850 hPa wind, vertically integrated moisture flux 925–850 hPa ($kg^2m^2s^{-2} \times 10^3$), and 200 hPa wind during conditions of (a) high TNA and high tropical Pacific SSTs, (b) low TNA and low tropical Pacific SSTs, (c) low TNA and high tropical Pacific SSTs, and (d) high TNA and low tropical Pacific SSTs. Wind vector arrows in lower right corner of wind plots indicate vector magnitude in ms-1. Boxes indicate 5 × 5 degree region containing study area.

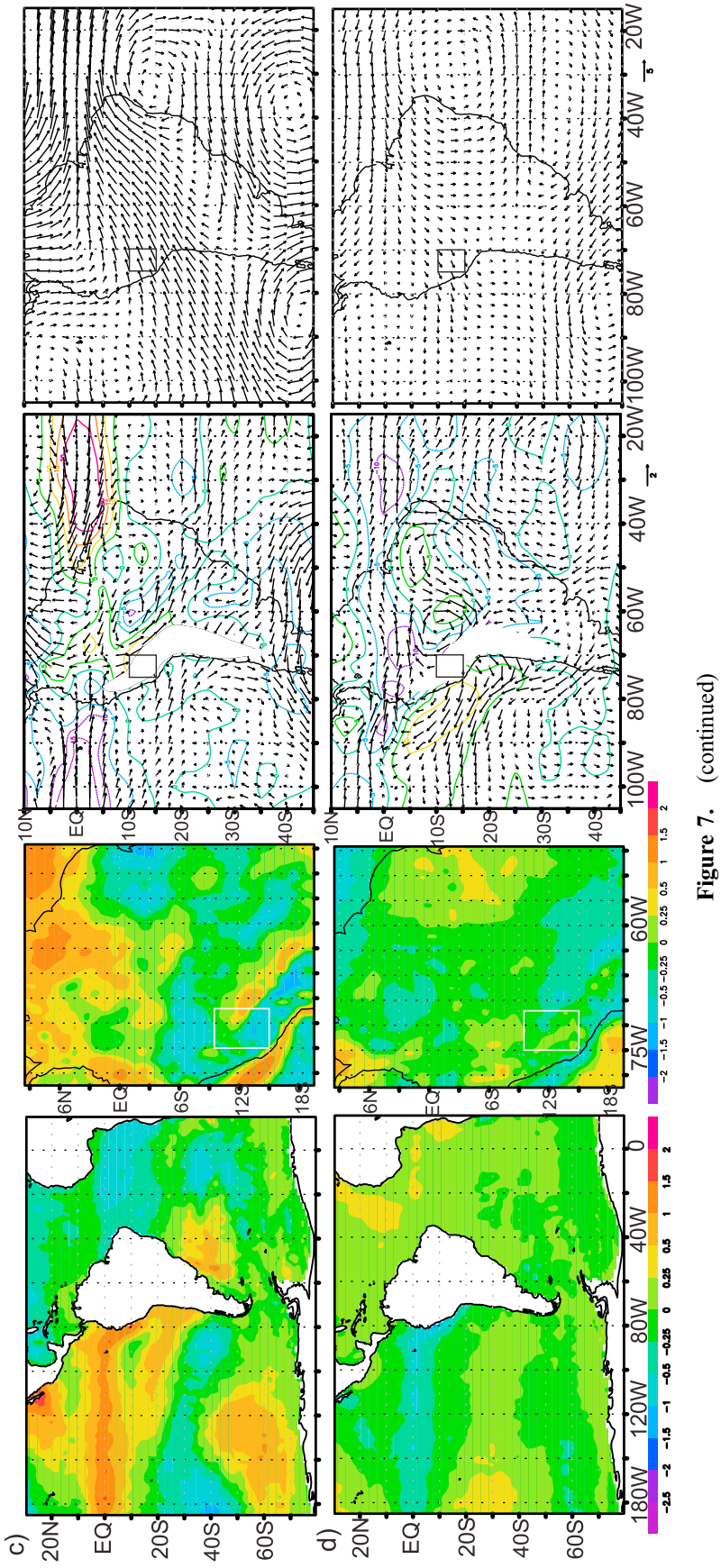

Figure 7. (continued)

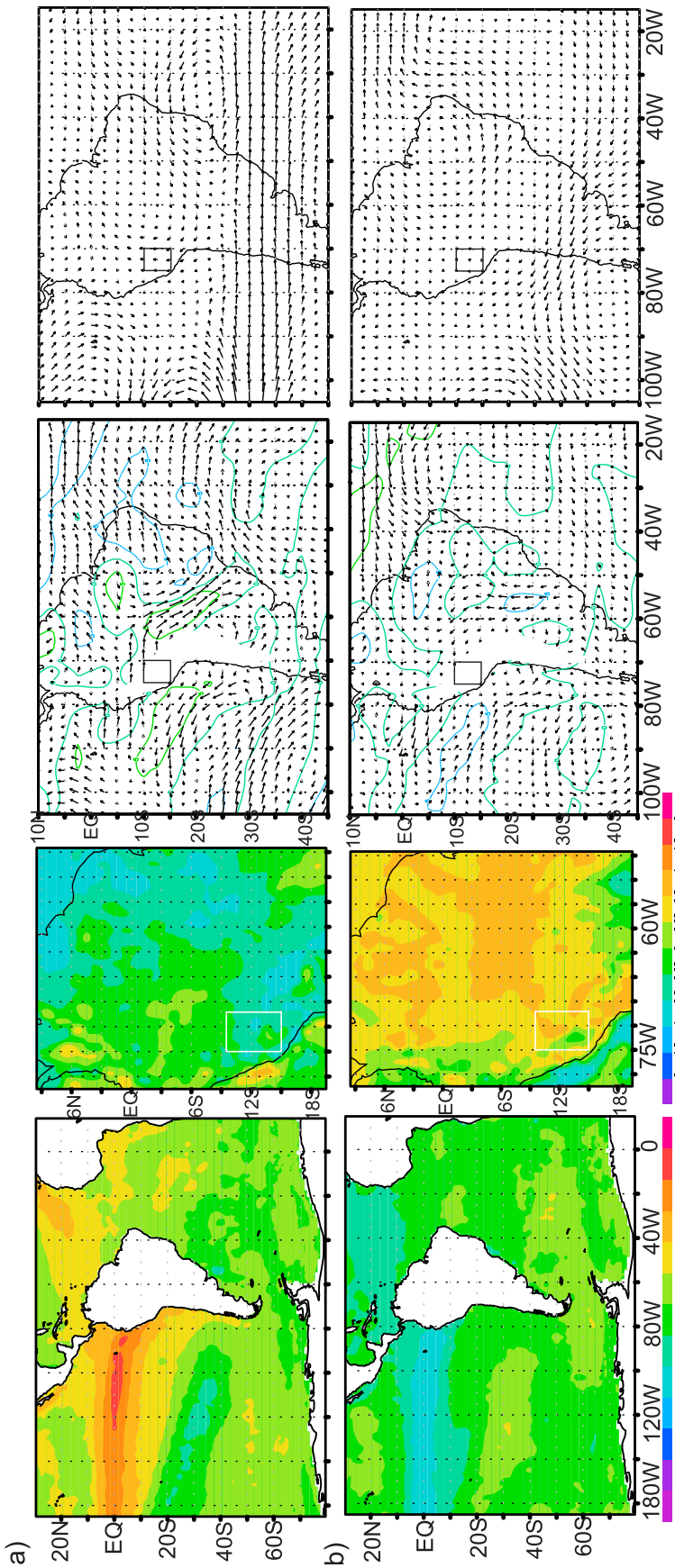

Figure 8. SON anomalies for HadISST (3-month moving average applied),ISCCP cloud frequency, NCEP/NCAR reanalysis 850 hPa wind, vertically integrated moisture flux 925–850 hPa (kg2m2s-2 × 103), and 200 hPa wind during conditions of (a) high TNA and high tropical Pacific SSTs, (b) low TNA and low tropical Pacific SSTs, (c) low TNA and high tropical Pacific SSTs, and (d) high TNA and low tropical Pacific SSTs. Wind vector arrows in lower right corner of wind plots indicate vector magnitude in ms-1. Boxes indicate 5 × 5 degree region containing study area.

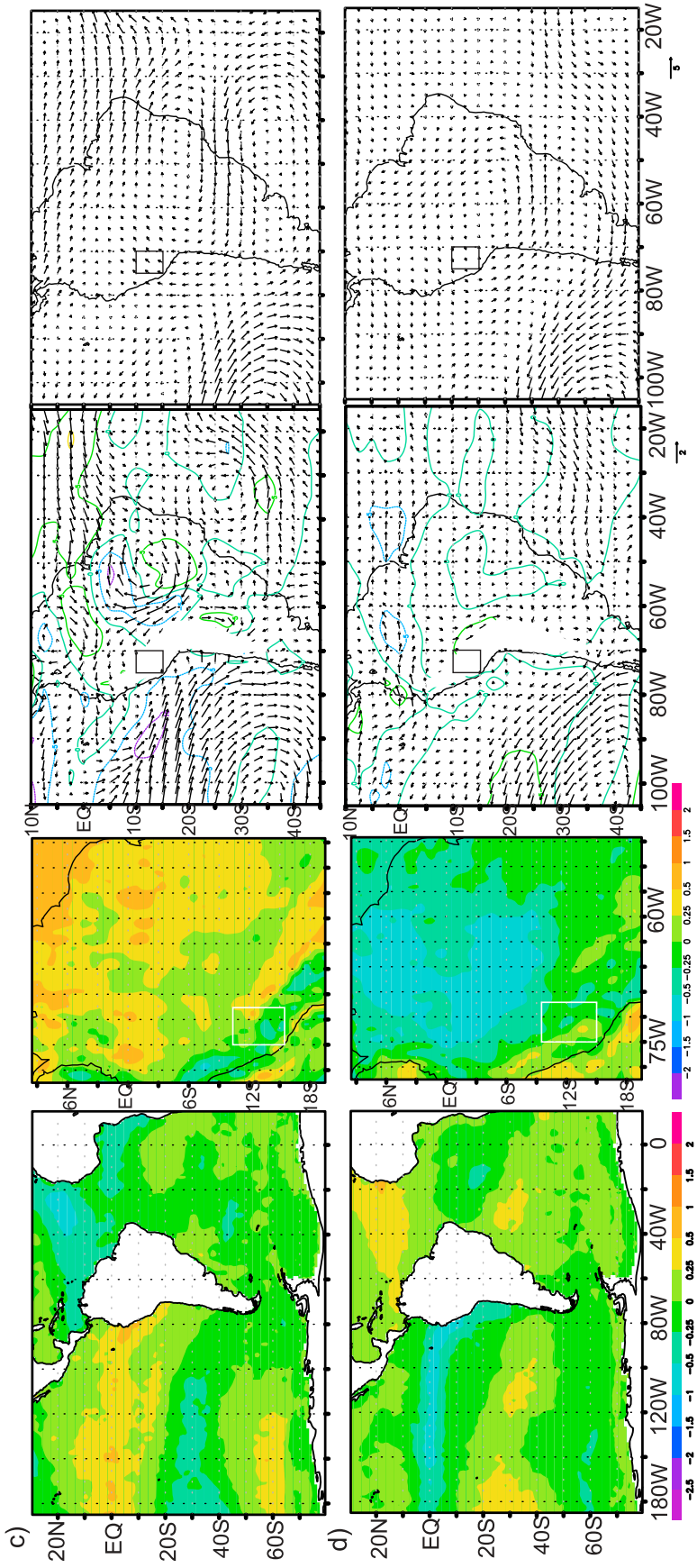

Figure 8. (continued)

Table 2. SST Anomalies for the Tropical Pacific and TNA in °C, Cloud Frequency Anomalies for Three Zones, Direction of Low-Level and Upper-Level Circulation Anomalies, Sign of Moisture Flux Anomaly (Associated With Trajectory of Low-Level Flow) and Number of Seasons Included in Composite[a]

	SSTs		Cloud Freq.			Wind			
	TP SSTa	TA SSTa	lowl	eslp	puna	Circ. (Upp)	Circ. (Low)	M. Flx (Low)	No. Seas.
DJF	0.71	0.26	*−0.16*	*−0.11*	*−0.08*	W		−	5
	−0.45	*−0.24*	0.19	0.17	0.16	E	E		5
	0.62	*−0.22*	0.00	*−0.10*	*−0.25*	W	E		2
	−0.59	0.18	*−0.08*	0.03	0.01	E	SW		3
MAM	1.14	0.22	*−0.22*	*−0.38*	*−0.42*	W	NW		3
	−0.48	*−0.33*	0.27	0.37	0.36	E	E		3
	0.65	*−0.22*	0.13	*−0.18*	*−0.32*	W	NW	+	2
	−0.31	0.16	*−0.10*	0.08	0.01	E	SE	−	5
JJA	0.59	0.29	*−0.30*	*−0.28*	*−0.15*	E-	W	−	5
	−0.32	*−0.22*	0.09	0.17	0.11		E	+	8
	0.26	*−0.22*	0.13	*−0.12*	*−0.04*	W		+	3
	−0.16	0.20	0.08	*−0.08*	0.19	W−	NW		3
SON	0.81	0.28	*−0.17*	*−0.12*	*−0.05*		W−	−	5
	−0.41	*−0.23*	0.18	0.10	0.09				7
	0.26	*−0.23*	0.11	0.00	*−0.10*	SW−		+	5
	−0.27	0.21	*−0.09*	*−0.03*	0.00		NW−		5

[a]Negative anomalies are italicized.

anomalies in the study area which extend into northern and eastern Brazil, which may explain the correlation between lowland cloud frequency and TNA SSTs. Alternatively, the high TNA SST anomalies may be associated with increased subsidence [*Marengo et al.*, 2008]. The two areas of increased cloud frequency at around 13 and 17°S may result from increased nocturnal convection when katabatic flows and moist lowland air converge as is known to occur in Ecuador [*Bendix et al.*, 2009].

[30] In SON (Figure 8) as in MAM, there are clear patterns of high (low) cloud frequency associated with low (high) SST anomalies in both basins. However, in contrast with MAM, the upper level circulation anomalies are very weak. With opposite anomalies in the two basins, cloud frequency anomalies follow the sign of TNA SST anomalies in the lowlands. In the high (low) TNA SST composites, there are weakened (strengthened) northeast trades in northern Brazil, consistent with the low (high) cloud frequencies in the lowlands and to a lesser extent in the other zones. High TNA SSTs and weakened northeast trades are thought to have played a role in the Amazon drought of 2005 [*Marengo et al.*, 2008]. Northeast Brazil is crossed by the mean low-level wind trajectory for the study area in this season. Therefore, this could account for the low cloud frequencies, as in the late dry season, the area is likely to be more dependent on moisture transport from the northern Amazon where rainfall is less seasonal. The lack of strong circulation anomalies suggests that other factors may be involved, for example, the duration and intensity of the early to mid dry season.

[31] Anomaly maps for DJF and JJA were also generated (not shown) but the results are summarized in Table 2. In DJF there are strong upper level circulation anomalies as in MAM with which the SST anomalies in the TNA and tropical Pacific are consistent. In both JJA and DJF, high (low) SST anomalies in both basins are associated with widespread low (high) cloud frequency anomalies. In DJF, with opposite sign anomalies in the TNA and tropical Pacific, the lowland cloud frequencies were negative with high TNA SSTs while the eastern slope and puna followed the tropical Pacific. In JJA the pattern for opposite sign anomalies was less clear.

4. Trends in Cloud Frequency

4.1. Regional Trends

[32] Figure 9 shows the widespread decreasing trends in mean annual cloud frequency across northern South America, apart from in the far western lowlands and Andes of Ecuador and the northeast fringes of the Amazon, where trends are not significant at the 10% level or are increasing. Areas with strongest decreasing trends are toward the central and southwestern Amazon, along the Andes of Colombia and in the far south, but east of the Andes. A few areas, mostly in the high Andes, show increasing trends. These are areas of high cloud frequency and low variability [*Halladay et al.*, 2012] which may indicate a resilience to the drivers of widespread decreases elsewhere. (Note that the strong decreasing trends near the coast of southern Peru to the west of the Andes will not be considered for the purposes of this study as the correction procedure employed was not applicable to this region).

[33] When split by month, trends were significant in all months although the spatial distribution of the trends is variable throughout the year (Figure 10). At the end of the southern hemisphere wet season and into the start of the dry season (March to June and August) there were strong decreasing trends in the southwest, which extend northwestward in February and June. In January, August and October there were decreasing trends in the central northern region as in the annual trend map. In September, the significant trends occur mostly to the west and appear to coincide with the eastern flank of the Andes. Of primary interest to this study are the trends in cloud frequency for the Andes/Amazon transition zone in southeastern Peru. The significant trends in this region occur in January, March, May and September.

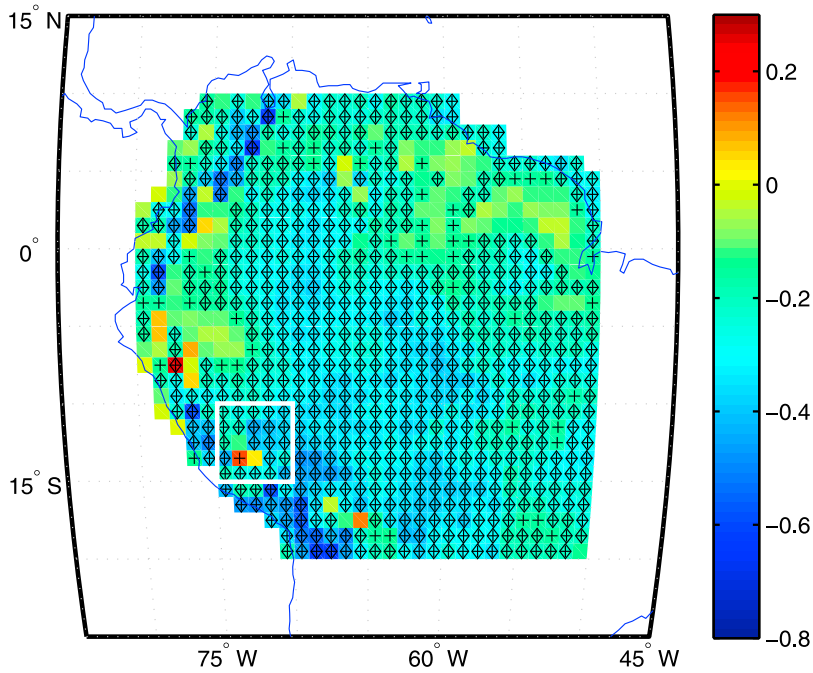

Figure 9. Trends in annual cloud frequency 1983–2008 at 1 × 1 degree resolution based on standardized anomalies. Plus signs (diamonds) indicate trends significant at the 10% (5%) level. Trends are plotted in s.d. units per decade. Five × 5 degree area containing study area is marked with a white border.

[34] In January, a decrease in cloud frequency would have little impact on the TMCF ecosystem as the mean cloud frequency and rainfall are high, but in March, May or September, a reduction in cloud frequency would have the potential to increase the length and/or intensity of the dry season. The occurrence of widespread decreasing trends over the SW Amazon in May, would have the greatest potential impact as they occur over a broad area of low mean cloud frequency for that month [see *Halladay et al.*, 2012, Figure 3].

4.2. Trends in the Study Area

[35] Cloud frequencies have decreased for all three zones (Figure 11), but only the trend of −0.38 s.d. units per decade for the lowlands is significant (at the 1% level), which is equivalent to a 2% reduction in cloud frequency. This is equivalent to the zonal mean decrease in cloud fraction at this latitude from ISCCP [*Zhou et al.*, 2011] after all regions with large viewing angles have been excluded. Comparison with Figure 9 suggests that the puna may include the region with an increasing trend at around 13°S, 73°W whereas the lowlands are part of the widespread regional decreasing trend.

[36] Examination of the trends by month for the three zones (Table S3 in the auxiliary material) reveals that for the lowlands there were significant decreases in January, March and September (at the 5% level) and in May and August (at the 10% level). In April the trend is also negative but not significant. For the eastern slope there was a significant decreasing trend at the 10% level in March but for the puna there were no significant trends.

[37] Trends plotted by month and hour for the lowlands indicate that decreasing trends in January, March and September were spread throughout the day (Figure 12). However, significant trends at 07 LT were present in each month from January to May, and in August, September and November. The magnitude of 07 LT trend ranged from 0.04 (March) to 0.08 (September), which represented reductions of 4 to 8% in cloud frequency. For the eastern slope there were significant decreases at 07 and 19 LT in March. For the puna, there was one significant increasing trend in July.

[38] In order to substantiate the cloud frequency trends from ISCCP, data from 2000 onwards were compared with MODIS MOD35 (at 15Z) and observations from the Rocotal and Chontachaca stations (at 12Z and 18Z). The trends were compared for these three times of day, for the three zones and by month. Of the 39 trends that were significant at the 10% level in any of the three data sets, 33 were replicated by another data set, i.e., a trend of the same sign was present.

4.3. Dry Season Length and Intensity

[39] Cloud frequency is particularly important in TMCF ecosystems in the dry season as it provides a significant moisture input. Therefore, it is useful to also examine trends in dry season length and intensity, in order to investigate the possibility of increased exposure to water stress.

[40] The statistics relating to the dry season were generated from a 20-day moving average of the daily ISCCP cloud frequency time series. First, the anomaly time series was created, then the number of days of low cloud frequency was calculated as the total days with anomaly cloud frequency less than the mean for each year. The intensity is the sum of cloud frequency anomalies for all days below the mean. Start (and end) days for the season were defined as the first crossing of the mean by the cloud frequency anomaly curve from positive (negative) to negative (positive), and the length as the difference between the two. Each statistic was calculated for each year excluding those with missing data at the

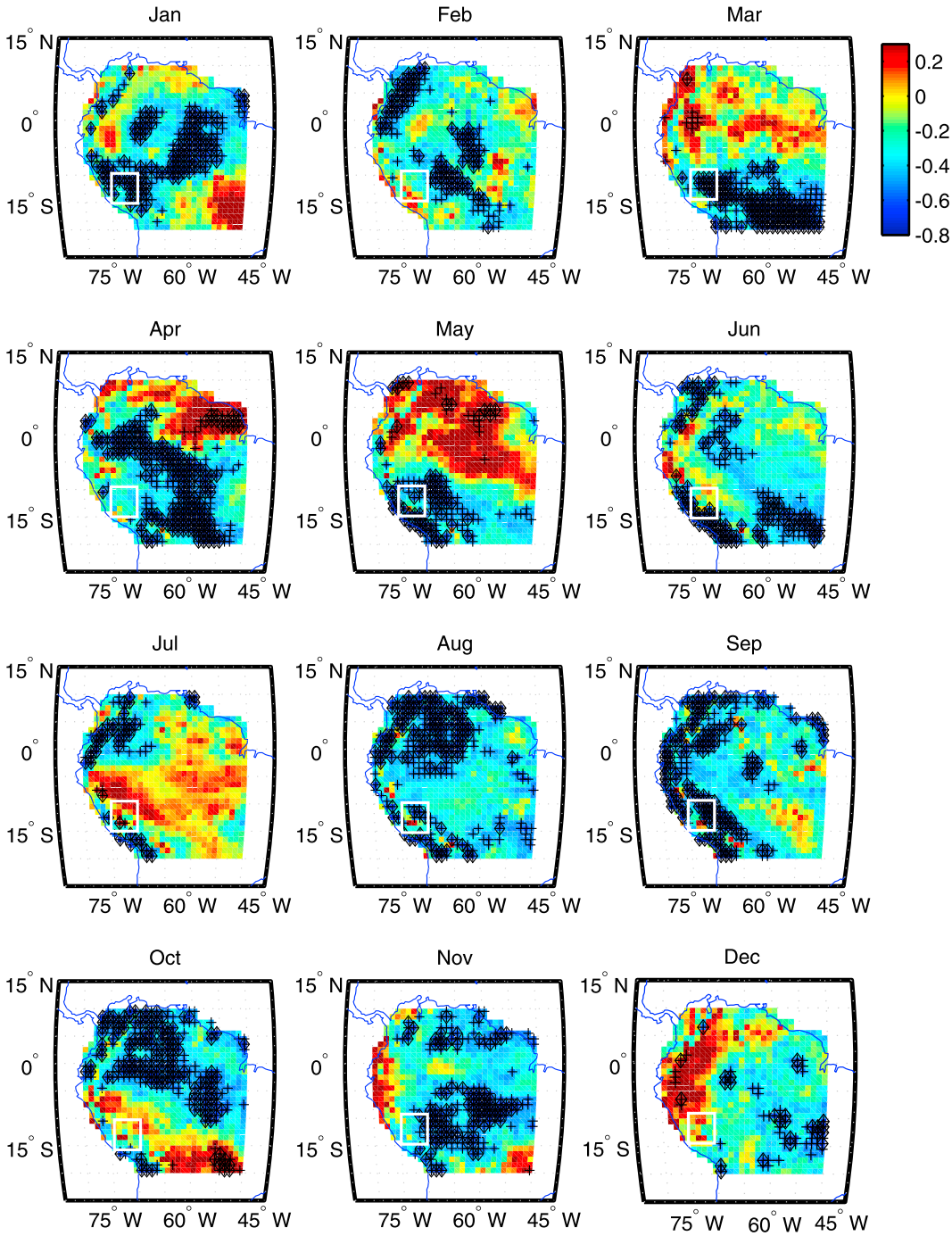

Figure 10. Trends in standardized anomaly cloud frequency by month 1983–2008 at 1 degree × 1 degree resolution. Plus signs (diamonds) indicate trends that are significant at the 10% (5%) level. Trends are plotted in s.d. units per decade. Five × 5 degree area containing study area is marked with white border.

start or end of the dry season, or both. A significant increasing trend in dry season intensity and a trend toward an earlier start day were found for the lowlands (Table 3). It should be noted that the number of days with low cloud frequency was equal to dry season length for years in which the start and end were well-defined, but not for years in which the cloud frequency fluctuated around the mean at the start or end of the dry season (i.e., start and end were poorly defined).

4.4. Trends in Related Observations

4.4.1. SSTs

[41] Over the period of the ISCCP data set there were significant increasing annual trends in SSTs in the TNA, South Pacific Anticyclone and Indian Ocean (Table S4 in the auxiliary material). The increases are significant in all months in the TNA region. As shown in previous sections, above normal SSTs in most regions are associated with decreased

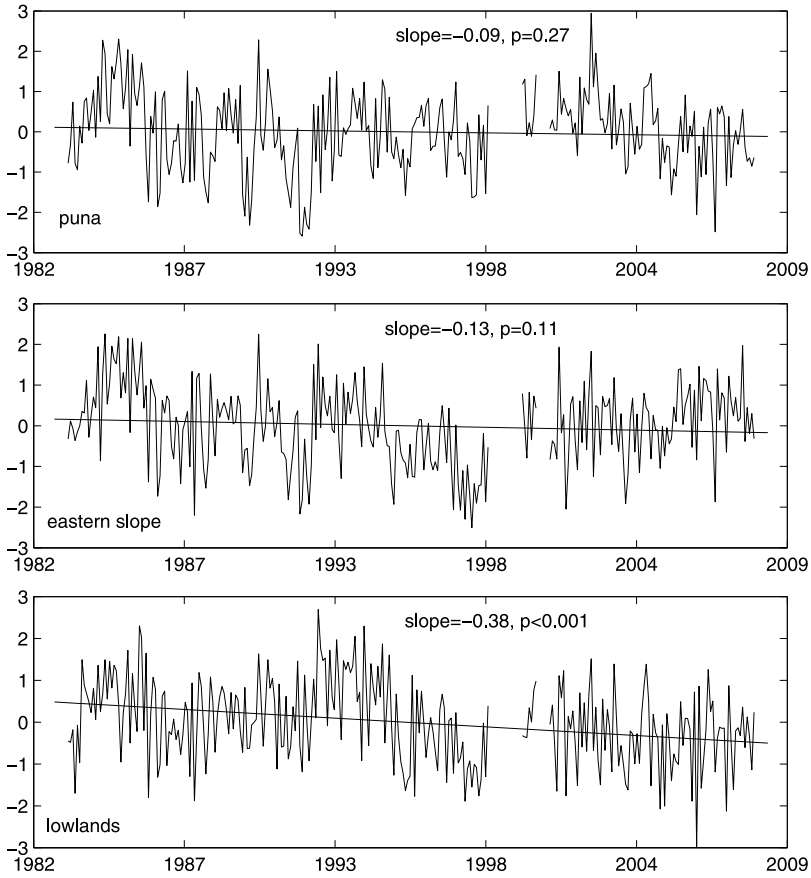

Figure 11. Monthly time series and linear trend in ISCCP standardized cloud frequency anomalies for 3 zones 1983–2008 (from 5 × 5 degree box) with slope and p-values for the trend (per decade). *y* axis in s.d. units based on monthly values.

cloud frequency. The correlation between TNA SSTs and lowland cloud frequencies for five months of the year and the significant trends in both strengthens the case for a connection. Similarly, the mixed sign, non-significant trends on the puna fit with its correlation with SSTs in the Pacific and Indian Oceans.

4.4.2. Other Observations

[42] Records of sunshine hours offer a verification method for estimates of cloud cover. *Raichijk* [2012] reported an increase in sunshine duration in equatorial regions of South America (approximates to areas of Brazil between 12°S and 2°N) for the period 1990–2004, which in turn suggests that cloud cover has reduced in this area over the same period.

[43] Figure 13 illustrates an increasing trend in the magnitude of the low level (850 hPa) zonal wind in the central Amazon, which equates to an enhanced westerly component or weakening of the easterly trades. As has been shown in the 850 hPa wind plots in Section 3.3, high cloud frequencies are commonly associated with enhanced easterlies and low cloud frequencies with weak easterlies in the lowlands to the east of the study area. The time series of low-level zonal wind exhibits considerable interannual variability, however, the high values are concentrated in the period from 2002 onwards, which is the period of sustained above normal SST anomalies in the TNA (Figure 6).

[44] Another parameter that suggests reduced cloud frequency is an increase in the diurnal temperature range (DTR) [*Dai et al.*, 1997]. With reduced cloud cover overnight, less of the outgoing longwave radiation from the ground is reflected back; thus, the nighttime minimum temperature is lower. Maximum and minimum temperature data were available for the period June 1995 to December 2006 from a weather station at Tambopata (13.13°S, 69.61°W). Increasing trends were found in March, August and September, which were significant at just outside the 10% level. However, the highest DTR anomalies in August and September occurred in the same years as the highest SST anomalies in the tropical Atlantic.

5. Discussion

[45] Analysis of the influence of SST areas indicates that cloud frequency on the puna is influenced predominantly by Pacific SSTs, and the lowlands by TNA SSTs. This pattern has previously been shown for convective cloud/rainfall in studies concentrating on either the central Andes/Altiplano [e.g., *Vuille et al.*, 2000] or the Amazon Basin [e.g., *Marengo*, 1992; *Marengo et al.*, 2008], but the influences on the transitional eastern slope have not been examined. It is possible that the decoupling of puna and lowlands described above is greatest in the late dry season because SSTs are reaching a maximum in the TNA, *and* lowland cloud frequencies are more strongly correlated with TNA SSTs than those on the puna at this time. Linear correlation of cloud frequency and SSTs suggests that

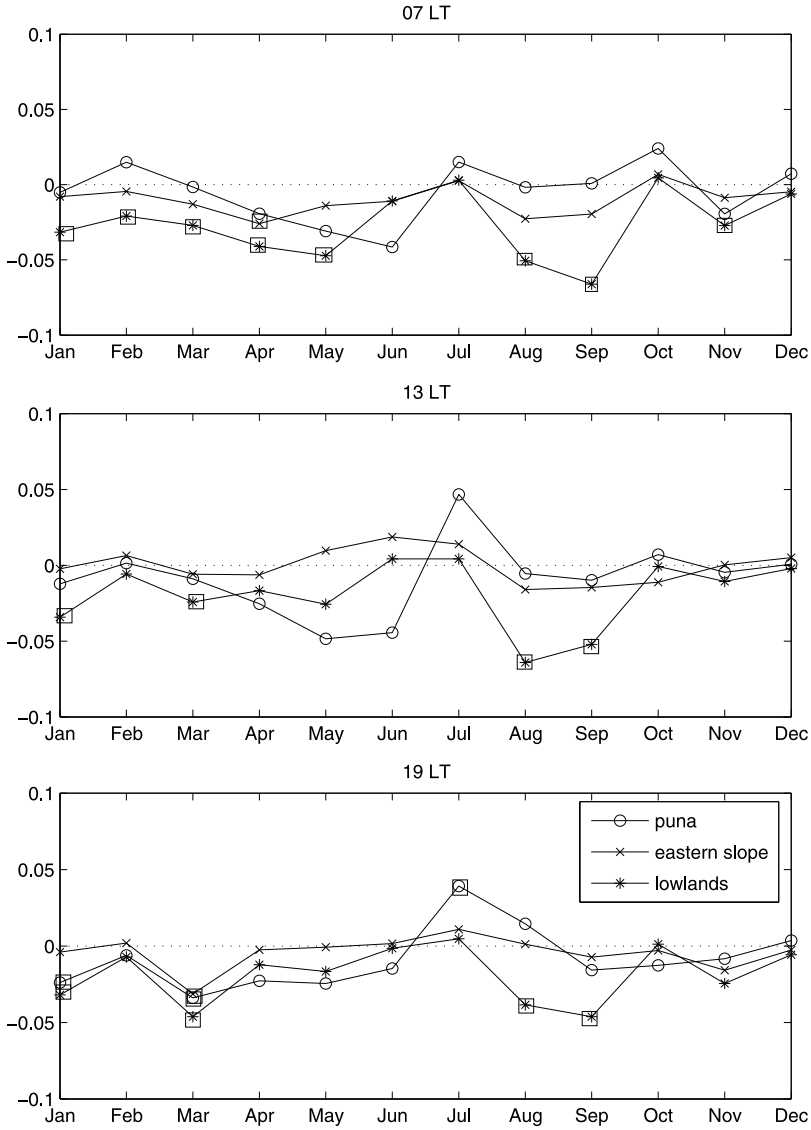

Figure 12. Linear trends in cloud frequency by month and hour per decade averaged over three times of day, centered on 07 LT, 13 LT and 19 LT for lowland, eastern slope and puna. Trends with associated p-values significant at the 10% level are indicated by squares.

the Pacific SST influences on the eastern slope are dominant, as for the puna. The analyses of central Andes precipitation and temperature undertaken by *Vuille et al.* [2000] also found that above 1500 m (equivalent to the lower eastern slope), Atlantic SSTs had no influence. However, these analyses included only summer temperature and precipitation.

[46] Notably, eastern slope cloud frequency anomalies peaked in September 2005 and 2006, but were low for the lowlands and puna at these times. These periods also coincided with positive SST anomalies in the TNA. This may suggest that the eastern slope area is more climatically stable than the puna and the lowlands on account of the orographic cloud formation as opposed to a reliance on low-level convergence, moisture transport or convective motion, even in the case of enhanced subsidence related to high SSTs. Low-level convergence of nighttime downslope flows and synoptic easterlies is thought to be an important cloud formation mechanism in the lowlands and at lower elevations on the eastern slope

Table 3. Linear Trends per Decade and p-Values for Number of Days With Cloud Frequency Below Mean, Dry Season Intensity Calculated From the Sum of Negative Cloud Frequency Anomalies, Start and End Day of the Dry Season, and Length Based on Number of Days From Start to End Day for Three Zones for the Period 1984 to 2007[a]

	Puna		Eastern Slope		Lowlands	
	Trend	p	Trend	p	Trend	p
Days low cloud freq	−4.44	0.63	3.17	0.64	7.86	0.16
Intensity	0.35	0.91	0.46	0.79	**4.46**	**0.02**
Start day	4.46	0.57	−2.37	0.48	**−8.19**	**0.06**
End day	−11.37	0.24	−4.43	0.65	0.19	0.97
Length	−15.83	0.23	−2.06	0.85	8.38	0.20

[a]Values in bold indicate trends significant at the 10% level.

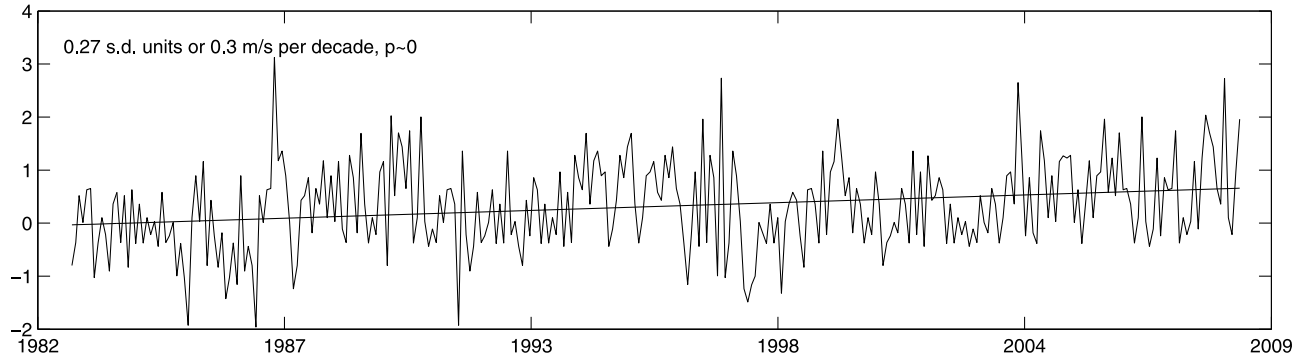

Figure 13. NCEP/NCAR reanalysis zonal wind at 850 hPa standardized anomaly time series with linear trend for 0 to 10°S, 70 to 60°W 1983–2008. *y* axis units are s.d. units.

[e.g., *Giovannettone and Barros*, 2009; *Killeen et al.*, 2007]. Although the SST controls on cloud frequency were similar for the puna and the eastern slope, vegetation and soil moisture content on the eastern slope may buffer instances of reduced moisture import via large scale flow, and enhance cloud formation. Lower variance on the eastern slope is supported by *Halladay et al.* [2012]. However, in years of extreme variability such as the 1998 El Niño, the highly modified large-scale circulation could overcome any relative stability afforded by the cloud formation mechanism or environmental buffering, leading to low cloud frequency anomalies in all three zones. It is also possible that convective activity and cloud cover over the South American continent may in turn modulate SSTs, though lag/lead correlations did not show any clear patterns that would be indicative of this.

[47] Analysis of ISCCP DX data for cloud frequency trends 1983–2008 suggested that there were widespread decreasing trends across northern South America. However, there is some uncertainty in the trend calculations from satellite calibrations, due to viewing angle changes and uncertainty in cloud detection algorithms themselves. Nonetheless, the decreasing trends are supported by results from other studies. For example, *Arias et al.* [2011] corroborated decreasing trends in high cloud over the central Amazon in DJF and SON with similar trends in OLR. Their results also show significant decreasing trends in high cloud over the study area (and much of the SW Amazon basin) in MAM, in common with this study.

[48] The pattern of trends in this study is not dissimilar from that of precipitation trends for the Amazon shown in *Malhi and Wright* [2004] in which there are decreases in the northwest and increases in the northeast; however, these results refer to the period 1960 to 1998. An overall decreasing trend for cloud frequency in South America was also found by *Warren et al.* [2007] using only ground-based observations for the period 1971 to 1996.

[49] Comparisons between the cloud frequency trend maps by month and the trends by month for the three zones with the results of *Butt et al.* [2009] showed agreement in terms of the existence of increasing trends in April and May in the northern Amazon, widespread decreases in June and August, and increases in the southwest Amazon in October. For the southwest region in *Butt et al.* [2009], which contains the study area, a significant increasing trend was found only in October, whereas in this study there were significant decreases in January, March and September. There are several possible reasons for the discrepancy. The times of days used by *Butt et al.* [2009] are centered on 09, 12 and 15 LT, whereas this study uses all times of day, with a lower weighting applied to the time steps either side i.e., the 07 LT data has a lesser influence than in this study. Given that many of the significant trends in this study were found to occur at 07 LT (Figure 12), a lower weighting for this time would reduce the magnitude of a decreasing trend. Second, the areas used in *Butt et al.* [2009] are not directly comparable with the much smaller domains used to represent the three zones in this study. Third, this study used a viewing angle correction procedure that takes into account the changes in viewing angle with time, whereas *Butt et al.* [2009] used a correction which did not take this into account.

[50] Many of the significant decreasing trends in the lowlands occurred in the early morning. However, these results are treated with caution as the number of significant trends (when split by month and hour) is not much more than would be expected by chance. Decreases in early morning cloud may be associated with changes in low-level convergence of katabatic flows with synoptic easterlies in the lowlands, though further investigation would be required to confirm this.

[51] *Malhi et al.* [2009] report that a reduction in dry season rainfall and extension of the dry season is predicted to occur with global warming in accordance with dry season intensity trends found in this study, moreover, modeling experiments by *Harris et al.* [2008] have attributed this to increases in Pacific and Atlantic SSTs. It is likely that the decreases in cloud frequency are caused by the same mechanism which was shown to be increased ascent over warm SSTs and descent over Amazonia. *Cox et al.* [2008] confirm the relationship between western Amazon rainfall and Atlantic SSTs, specifically, the gradient between the north and south equatorial Atlantic.

6. Conclusions

[52] We have examined covariability and interannual variability of cloud frequency in puna, eastern slope and lowland zones, trends, and possible controlling mechanisms at the Andes/Amazon transition in southeastern Peru. The main conclusions are as follows:

[53] 1) Correlations coefficients for monthly cloud frequency between the three zones are significant except in the late dry season.

[54] 2) Cloud frequency on the puna is influenced predominantly by Pacific SSTs, and the lowlands by TNA SSTs.

The eastern slope appeared most affected by Pacific SSTs but SST correlations were reduced overall compared with the other zones.

[55] 3) High (low) SST anomalies in both the tropical Pacific and TNA are associated with low (high) cloud frequency anomalies across tropical South America and in all 3 zones.

[56] 4) ISCCP DX data for cloud frequency trends 1983–2008 suggested that there were widespread decreasing trends across northern South America.

[57] 5) Within the study area, a significant decreasing trend has occurred in the lowlands in January, March and September (at the 1% level). On the eastern slope, there was a significant decreasing trend in March (at the 5% level).

[58] 6) Correlations between the cloud frequency time series and various SST regions suggested that the decreasing trends in cloud frequency in the late dry season over the lowlands may be associated with increasing SSTs in the TNA and Indian Ocean. Inclusion of the trend in the correlations with TNA SSTs increased r substantially for the lowlands in some months but late dry season r values remained high, with and without trends.

[59] 7) Many of the most significant decreasing trends for the lowlands and to a lesser extent on the eastern slope tend to occur in the early morning.

[60] 8) A significant increasing trend in dry season intensity was found for the lowlands.

[61] The decreasing cloud frequency trends, increased dry season intensity and correlation with TNA SSTs imply that droughts may become more frequent in the lowlands. HadCM3 projections suggest that the relationship between western Amazon rainfall and Atlantic SSTs will strengthen as aerosol pollution in the northern hemisphere reduces [*Cox et al.*, 2008]. The cooling effect of aerosols has partially offset the warming associated with GHGs [*Andreae et al.*, 2005]. *Cox et al.* [2008] suggest that the combination of reduced aerosol pollution and increased GHG concentrations will result in the probability of 2005-level droughts increasing to 1-in-2 by 2025. Indeed, the extent of the 2010 drought in Amazonia of comparable or even greater severity than 2005 is now beginning to emerge [e.g., *Lewis et al.*, 2011; *Marengo et al.*, 2011]. Therefore, the occurrence of low cloud frequency anomalies is also likely to increase. If the predicted rise in tropical Pacific SSTs is to occur, then the same is likely to occur on the eastern slope and the puna. In addition, current and future environmental changes are not restricted to climate and meteorology but also include land use changes e.g., loss of forests and replacement with pasture, which affects latent heat partitioning and cloud formation in TMCF ecosystems [*Ray et al.*, 2006], which may place the region under an even greater threat.

[62] Although this study indicated that increased SSTs in the TNA may be associated with reduced cloud frequency in the lowlands Andes/Amazon transition zone in southeastern Peru, a causal relationship has not been established. A regional modeling study with accurate representation of clouds and forced with SSTs would be required to confirm the association and the differences across the transition zone. In addition, the question of trends in cloud height has not been investigated, but will be the subject of future work.

[63] **Acknowledgments.** We acknowledge NERC (NE/F00916X/1), Microsoft Research, John Fell Fund, N. Salinas Revilla, R. Chacon Campana, Z. Huaman Gutierrez (Senamhi, Cuzco), and Michael Green.

References

Andreae, M. O., C. D. Jones, and P. M. Cox (2005), Strong present-day aerosol cooling implies a hot future, *Nature*, *435*(7046), 1187–1190, doi:10.1038/nature03671.

Arias, P. A., R. Fu, C. D. Hoyos, W. H. Li, and L. M. Zhou (2011), Changes in cloudiness over the Amazon rainforests during the last two decades: Diagnostic and potential causes, *Clim. Dyn.*, *37*(5–6), 1151–1164, doi:10.1007/s00382-010-0903-2.

Bendix, J., K. Trachte, J. Cermak, R. Rollenbeck, and T. Nauss (2009), Formation of convective clouds at the foothills of the tropical eastern Andes (south Ecuador), *J. Appl. Meteorol. Climatol.*, *48*(8), 1682–1695, doi:10.1175/2009JAMC2078.1.

Butt, N., M. New, G. Lizcano, and Y. Malhi (2009), Spatial patterns and recent trends in cloud fraction and cloud-related diffuse radiation in Amazonia, *J. Geophys. Res.*, *114*, D21104, doi:10.1029/2009JD012217.

Cox, P. M., P. P. Harris, C. Huntingford, R. A. Betts, M. Collins, C. D. Jones, T. E. Jupp, J. A. Marengo, and C. A. Nobre (2008), Increasing risk of Amazonian drought due to decreasing aerosol pollution, *Nature*, *453*(7192), 212–215, doi:10.1038/nature06960.

Dai, A., A. D. DelGenio, and I. Y. Fung (1997), Clouds, precipitation and temperature range, *Nature*, *386*(6626), 665–666, doi:10.1038/386665b0.

Drumond, A., and T. Ambrizzi (2008), The role of the South Indian and Pacific oceans in South American monsoon variability, *Theor. Appl. Climatol.*, *94*(3–4), 125–137, doi:10.1007/s00704-007-0358-5.

Enfield, D. B., and D. A. Mayer (1997), Tropical Atlantic sea surface temperature variability and its relation to El Nino Southern Oscillation, *J. Geophys. Res.*, *102*(C1), 929–945, doi:10.1029/96JC03296.

Foster, P. N. (2001), The potential negative impacts of climate change on tropical montane cloud forests, *Earth Sci. Rev.*, *55*, 73–106, doi:10.1016/S0012-8252(01)00056-3.

Garreaud, R. D. (1999), Multiscale analysis of the summertime precipitation over the central Andes, *Mon. Weather Rev.*, *127*(5), 901–921, doi:10.1175/1520-0493(1999)127<0901:MAOTSP>2.0.CO;2.

Giovannettone, J. P., and A. P. Barros (2009), Probing regional orographic controls of precipitation and cloudiness in the central Andes using satellite data, *J. Hydrometeorol.*, *10*(1), 167–182, doi:10.1175/2008JHM973.1.

Halladay, K., M. New, and Y. Malhi (2012), Cloud frequency climatology at the Andes/Amazon transition: 1. Seasonal and diurnal cycles, *J. Geophys. Res.*, *117*, D23102, doi:10.1029/2012JD017770.

Harris, P. P., C. Huntingford, and P. M. Cox (2008), Amazon Basin climate under global warming: The role of the sea surface temperature, *Philos. Trans. R. Soc. B*, *363*(1498), 1753–1759, doi:10.1098/rstb.2007.0037.

Kalnay, E., et al. (1996), The NCEP/NCAR 40-year reanalysis project, *Bull. Am. Meteorol. Soc.*, *77*(3), 437–471, doi:10.1175/1520-0477(1996)077<0437:TNYRP>2.0.CO;2.

Killeen, T. J., M. Douglas, T. Consiglio, P. M. Jorgensen, and J. Mejia (2007), Dry spots and wet spots in the Andean hotspot, *J. Biogeogr.*, *34*(8), 1357–1373, doi:10.1111/j.1365-2699.2006.01682.x.

Lenters, J. D., and K. H. Cook (1999), Summertime precipitation variability over South America: Role of the large-scale circulation, *Mon. Weather Rev.*, *127*(3), 409–431, doi:10.1175/1520-0493(1999)127<0409:SPVOSA>2.0.CO;2.

Lewis, S. L., P. M. Brando, O. L. Phillips, G. M. F. van der Heijden, and D. Nepstad (2011), The 2010 Amazon drought, *Science*, *331*(6017), 554, doi:10.1126/science.1200807.

Liebmann, B., and J. A. Marengo (2001), Interannual variability of the rainy season and rainfall in the Brazilian Amazon basin, *J. Clim.*, *14*(22), 4308–4318, doi:10.1175/1520-0442(2001)014<4308:IVOTRS>2.0.CO;2.

Malhi, Y., and J. Wright (2004), Spatial patterns and recent trends in the climate of tropical rainforest regions, *Philos. Trans. R. Soc. B*, *359*(1443), 311–329, doi:10.1098/rstb.2003.1433.

Malhi, Y., L. Aragao, D. Galbraith, C. Huntingford, R. Fisher, P. Zelazowski, S. Sitch, C. McSweeney, and P. Meir (2009), Exploring the likelihood and mechanism of a climate-change-induced dieback of the Amazon rainforest, *Proc. Natl. Acad. Sci. U. S. A.*, *106*(49), 20,610–20,615, doi:10.1073/pnas.0804619106.

Marengo, J. A. (1992), Interannual variability of surface climate in the Amazon Basin, *Int. J. Climatol.*, *12*(8), 853–863, doi:10.1002/joc.3370120808.

Marengo, J. A., and S. Hastenrath (1993), Case-studies of extreme climatic events in the Amazon Basin, *J. Clim.*, *6*(4), 617–627, doi:10.1175/1520-0442(1993)006<0617:CSOECE>2.0.CO;2.

Marengo, J. A., C. A. Nobre, J. Tomasella, M. D. Oyama, G. S. De Oliveira, R. De Oliveira, H. Camargo, L. M. Alves, and I. F. Brown (2008), The drought of Amazonia in 2005, *J. Clim.*, *21*(3), 495–516, doi:10.1175/2007JCLI1600.1.

Marengo, J. A., J. Tomasella, L. M. Alves, W. R. Soares, and D. A. Rodriguez (2011), The drought of 2010 in the context of historical droughts in the Amazon region, *Geophys. Res. Lett.*, *38*, L12703, doi:10.1029/2011GL047436.

Mulligan, M., and S. M. Burke (2005), DFID FRP project ZF0216: Global cloud forests and environmental change in a hydrological context, final report, Dep. for Int. Dev., London.

Pinto, E., Y. Shin, S. A. Cowling, and C. D. Jones (2009), Past, present and future vegetation-cloud feedbacks in the Amazon Basin, *Clim. Dyn.*, *32*(6), 741–751, doi:10.1007/s00382-009-0536-5.

Pounds, J. A., M. P. L. Fogden, and J. H. Campbell (1999), Biological response to climate change on a tropical mountain, *Nature*, *398*(6728), 611–615, doi:10.1038/19297.

Raichijk, C. (2012), Observed trends in sunshine duration over South America, *Int. J. Climatol.*, *32*(5), 669–680, doi:10.1002/joc.2296.

Ray, D. K., U. S. Nair, R. O. Lawton, R. M. Welch, and R. A. Pielke Sr. (2006), Impact of land use on Costa Rican tropical montane cloud forests: Sensitivity of orographic cloud formation to deforestation in the plains, *J. Geophys. Res.*, *111*, D02108, doi:10.1029/2005JD006096.

Rayner, N. A., D. E. Parker, E. B. Horton, C. K. Folland, L. V. Alexander, D. P. Rowell, E. C. Kent, and A. Kaplan (2003), Global analyses of sea surface temperature, sea ice, and night marine air temperature since the late nineteenth century, *J. Geophys. Res.*, *108*(D14), 4407, doi:10.1029/2002JD002670.

Ronchail, J., G. Cochonneau, M. Molinier, J. L. Guyot, A. G. D. Chaves, V. Guimaraes, and E. de Oliveira (2002), Interannual rainfall variability in the Amazon basin and sea-surface temperatures in the equatorial Pacific and the tropical Atlantic Oceans, *Int. J. Climatol.*, *22*(13), 1663–1686, doi:10.1002/joc.815.

Rossow, W. B., and R. A. Schiffer (1991), ISCCP cloud data products, *Bull. Am. Meteorol. Soc.*, *72*(1), 2–20, doi:10.1175/1520-0477(1991)072<0002:ICDP>2.0.CO;2.

Rossow, W. B., and R. A. Schiffer (1999), Advances in understanding clouds from ISCCP, *Bull. Am. Meteorol. Soc.*, *80*(11), 2261–2287, doi:10.1175/1520-0477(1999)080<2261:AIUCFI>2.0.CO;2.

Vuille, M. (1999), Atmospheric circulation over the Bolivian Altiplano during dry and wet periods and extreme phases of the Southern Oscillation, *Int. J. Climatol.*, *19*(14), 1579–1600, doi:10.1002/(SICI)1097-0088(19991130)19:14<1579::AID-JOC441>3.0.CO;2-N.

Vuille, M., and F. Keimig (2004), Interannual variability of summertime convective cloudiness and precipitation in the central Andes derived from ISCCP-B3 data, *J. Clim.*, *17*(17), 3334–3348, doi:10.1175/1520-0442(2004)017<3334:IVOSCC>2.0.CO;2.

Vuille, M., D. R. Hardy, C. Braun, F. Keimig, and R. S. Bradley (1998), Atmospheric circulation anomalies associated with 1996/1997 summer precipitation events on Sajama ice cap, Bolivia, *J. Geophys. Res.*, *103*(D10), 11,191–11,204, doi:10.1029/98JD00681.

Vuille, M., R. S. Bradley, and F. Keimig (2000), Interannual climate variability in the Central Andes and its relation to tropical Pacific and Atlantic forcing, *J. Geophys. Res.*, *105*(D10), 12,447–12,460, doi:10.1029/2000JD900134.

Warren, S. G., R. M. Eastman, and C. J. Hahn (2007), A survey of changes in cloud cover and cloud types over land from surface observations, 1971–96, *J. Clim.*, *20*(4), 717–738, doi:10.1175/JCLI4031.1.

Xie, S. P., and J. A. Carton (2004), Tropical Atlantic variability: Patterns, mechanisms, and impacts, in *Earth's Climate: The Ocean-Atmosphere Interaction*, *Geophys. Monogr. Ser.*, vol. 147, edited by C. Wang, S.-P. Xie, and J. A. Carton, pp. 121–142, AGU, Washington, D. C., doi:10.1029/147GM07.

Yoon, J.-H., and N. Zeng (2010), An Atlantic influence on Amazon rainfall, *Clim. Dyn.*, *34*(2–3), 249–264, doi:10.1007/s00382-009-0551-6.

Zeng, N., J.-H. Yoon, J. A. Marengo, A. Subramaniam, C. A. Nobre, A. Mariotti, and J. D. Neelin (2008), Causes and impacts of the 2005 Amazon drought, *Environ. Res. Lett.*, *3*(1), 014002, doi:10.1088/1748-9326/3/1/014002.

Zhou, Y. P., K.-M. Xu, Y. C. Sud, and A. K. Betts (2011), Recent trends of the tropical hydrological cycle inferred from Global Precipitation Climatology Project and International Satellite Cloud Climatology Project data, *J. Geophys. Res.*, *116*, D09101, doi:10.1029/2010JD015197.